An Acad Bras Cienc (2025) 97(1): e20231254 DOI 10.1590/0001-3765202520231254
Anais da Academia Brasileira de Ciências | *Annals of the Brazilian Academy of Sciences*
Printed ISSN 0001-3765 I Online ISSN 1678-2690
www.scielo.br/aabc | www.fb.com/aabcjournal

GEOSCIENCES

The Borrachudos Granitic Suite: Paleo- to Mesoproterozoic A-type Magmatism in the Southeastern São Francisco Craton (SE Brazil)

IVO ANTONIO DUSSIN, MARIO LUIZ S.C. CHAVES, TANIA MARA DUSSIN, PHILLIPPE ROSSI & JACQUES CHARVET

Abstract: The Borrachudos Granitic Suite (BGS) comprises an acid magmatism that occurred in the west edge of Araçuaí orogen (Late Neoproterozoic), southeastern Brazil. Previous papers attributed the magma genesis to crustal thickening related to an older Paleoproterozoic, Transamazonian orogeny. However, geochronological data indicate that BGS is younger, dominated by about 1.7 Ga granitoids hosted in the archean basement. To investigate the nature of this magmatism, mineralogical, geochemical, Nd-Sr isotopic studies in the BGS and genetically related metarhyolites inside the fold belt were carried out. High SiO_2, K, Fe, F, Nb, Y, Zr and REE contents characterize granitoids and metarhyolites. The suite has $ENd_{(T)}$ values of -10.10 and -6.17, with T_{DM} of 2.6-3.0 Ga, and initial $^{87}Sr/^{86}Sr$ ratio of 0.7057, indicating features of alkaline and anorogenic (A-type) within plate granitic magmas, derived from a Proterozoic crustal source. Therefore, we argue that an orogenic model for this magmatism is not viable. We propose that BGS is associated to crustal melting induced by mantle diapirism or mantle derived magmas related to the Paleoproterozoic extensional tectonic that produced crustal rifting, westward, precursory to the Espinhaço Supergroup basin. Beryl- and topaz-rich pegmatites of NYF-type intruded the granites as well as nearby host gneisses during BGS evolution.

Key words: Borrachudos Suite, granitic magmatism, São Francisco Craton, southeastern Brazil.

INTRODUCTION

The "Borrachudos Granites" were so designated by Dorr & Barbosa (1963), outcropping to the northeast of the iron-rich mineral province known as Quadrilátero Ferrífero (Iron Quadrangle). A new designation, as "Borrachudos Suite" (Proterozoic undefined) was proposed by Grossi-Sad et al. (1990), together with another suite, the "Guanhães Suite" (Archean). Still in the 1990s, several authors recognized the Borrachudos Granitic Suite (BGS) as a type-A magmatism, that is alkaline and anorogenic (Dussin 1994a, b, Fernandes et al. 1994). Since the 1990s, there have few new studies on the subject.

The BGS is composed by several granite plutons that intrude a gneissified and migmatized basement of the tonalite-trondhjemite-granodiorite (TTG) archean association at the east margin of the Southern Espinhaço Range, southeastern Brazil (Fig. 1). The BGS outcrops mainly between the major towns of Itabira (to the south) and Guanhães (to the north), in the central region of the state of Minas Gerais. This group of lithologies occurs on the southeast side of the São Francisco Craton, a major tectonic unit that forms a broad nucleus stable since the Late Paleoproterozoic.

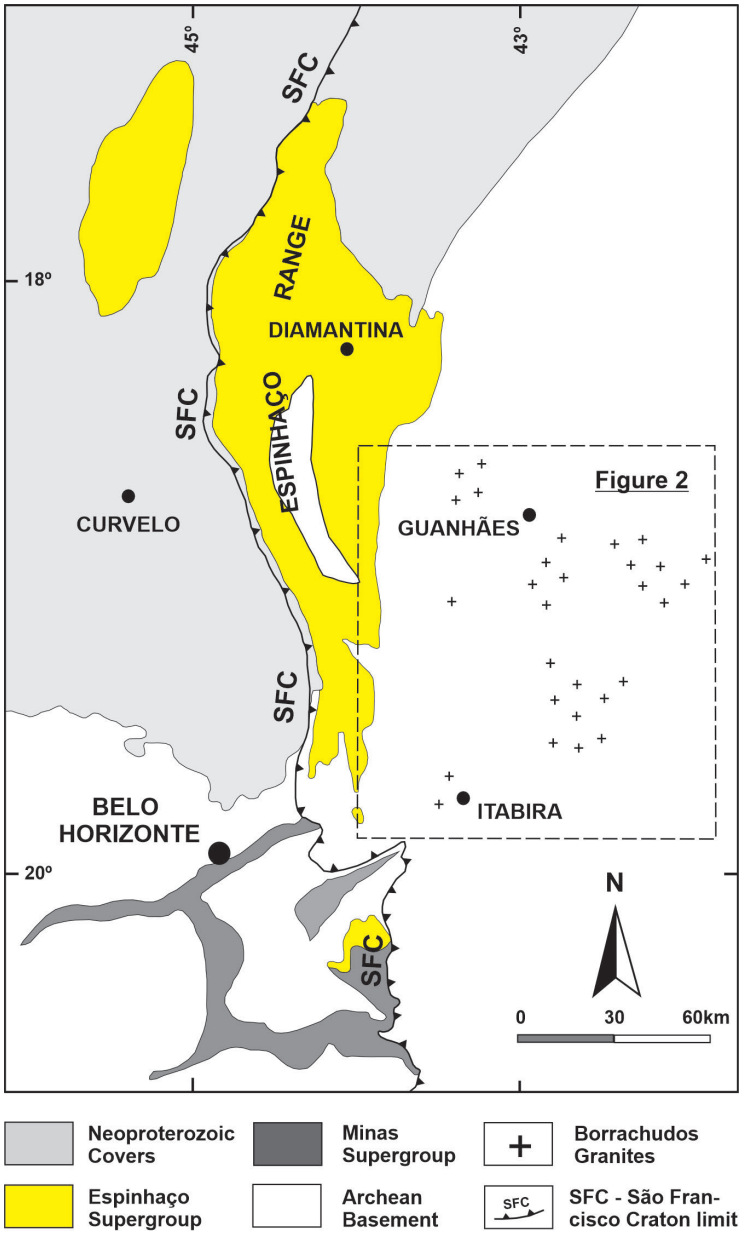

Figure 1. Schematic geologic map of the Southern Espinhaço and Quadrilátero Ferrífero region, southeastern São Francisco Craton, showing location of Fig. 2 (modified after Pinto & Silva 2014).

The São Francisco Craton at this present-day configuration can be characterized by edges remobilized during the Neoproterozoic, in the geotectonic Brasiliano Cycle at about 630 to 490 Ma (Pedrosa-Soares et al. 2011, Heilbron et al. 2017). The Araçuaí Orogen marks the southeastern boundary of the craton, although the role played by the Espinhaço Basin, and the Espinhaço Supergroup is still not well defined in this context. The Espinhaço Supergroup is formed mainly by clastic sequences of low metamorphic grade, whose greatest economic importance are the diamond-bearing conglomeratic deposits of the Sopa Brumadinho Formation (Chaves 1997, Chaves et al. 2001, Santos et al. 2013).

Geochronological data obtained from the Espinhaço Supergroup indicate that the opening of the basin took place around 1.71 Ga, according to dates obtained from acid metavolcanic rocks that occur at the base of the sequence, that is, on

the boundary between the Paleoproterozoic and Mesoproterozoic (Dussin 1994b, Chemale Jr. et al. 2012, Santos et al. 2013). Such age is analogous to those obtained for the BGS, ~1.7 Ga (Chemale Jr. et al. 1998), indicating the contemporaneity between both magmatic events.

The present study was undertaken to investigate the nature, geotectonic controls and origin of the BGS plutons and derived pegmatites, and the coeval acid metavolcanic rocks that occur at the base of the Espinhaço Supergroup.

BGS PREVIOUS KNOWLEDGE

Geological setting

In the western portion of the Araçuaí belt mainly gneisses and migmatites of Archean age are overlain by Proterozoic covers encompassing three sequences with different ages (Alkmim & Martins-Neto 2012, Santos et al. 2013, Alkmim et al. 2017). The oldest unit is a sedimentary succession including clastic deposits and banded iron formations of Paleoproterozoic age, which integrates the Minas Supergroup. Overlying this, the Paleo- to Mesoproterozoic Espinhaço Supergroup consists of thick quartzites and phyllites with local levels of conglomerates. Metarhyolites occur at the base of this sequence.

The Macaúbas Group, a sucession of clastic sediments with associated glaciogenic deposits, during the Neoproterozoic, complete the Precambrian sedimentary cycles in the region. All these units were deformed and metamorphosed during the Brasiliano Cycle (Uhlein 1991, Dussin 1994a, Pedrosa-Soares et al. 2011). Ductile deformation and associated metamorphism in the east of belt decrease westward, thus, rocks in the interior of the craton are few deformed and unmetamorphosed.

Granites in the southeastern part of the Espinhaço Range, to the northeast of the Quadrilátero Ferrífero, are intrusive into the Basement Complex. The country rocks are fine-grained ortho- and paragneisses interbanded with micaschists, ironstones and calc-silicate rocks.

The plutons, grouped into the Guanhães and Borrachudos suites, have distinctive chemical, petrographic and field characteristics (Grossi-Sad et al. 1990). The Guanhães Suite is represented by plutons of tonalitic to granodioritic composition, deformed probably during an orogeny of paleoproterozoic age (Siga Jr. 1986, Teixeira & Figueiredo 1991, Noce et al. 2000).

In the BGS seven plutons of the BGS were recognized by Dossin (1994a) – the São Félix, Senhora do Porto, Urubú, Açucena, Itabira, Itauninha and Peti plutons (Fig. 2). These bodies intrude Archean granite-gneiss complex, however they intrude no Proterozoic sedimentary sequences. There are no records of mafic magmatism coexisting with the BGS, and no exposed intermediate members of any differentiation series. Major NNW and NNE structural lineaments are associated with the plutons, and lineaments trending parallel to the principal axis of the sedimentary basins toward the west, within the Espinhaço belt, suggest a genetic relation between crustal fracturing and granite emplacement.

High-level intrusion is suggested by the sharp contacts with the host rocks, and by chilled margins many meters wide. A magmatic foliation within the plutons, marked by strong parallelism of amphibole and biotite, is parallel to the granite contacts, and a N-S lineation within the foliation is marked by the long-axes of mafic minerals. Crystal breakage perpendicular to the lineation is related to tensional deformation in the diapirs; the features are filled by quartz and biotite, indicating its formation in an only partly solid state.

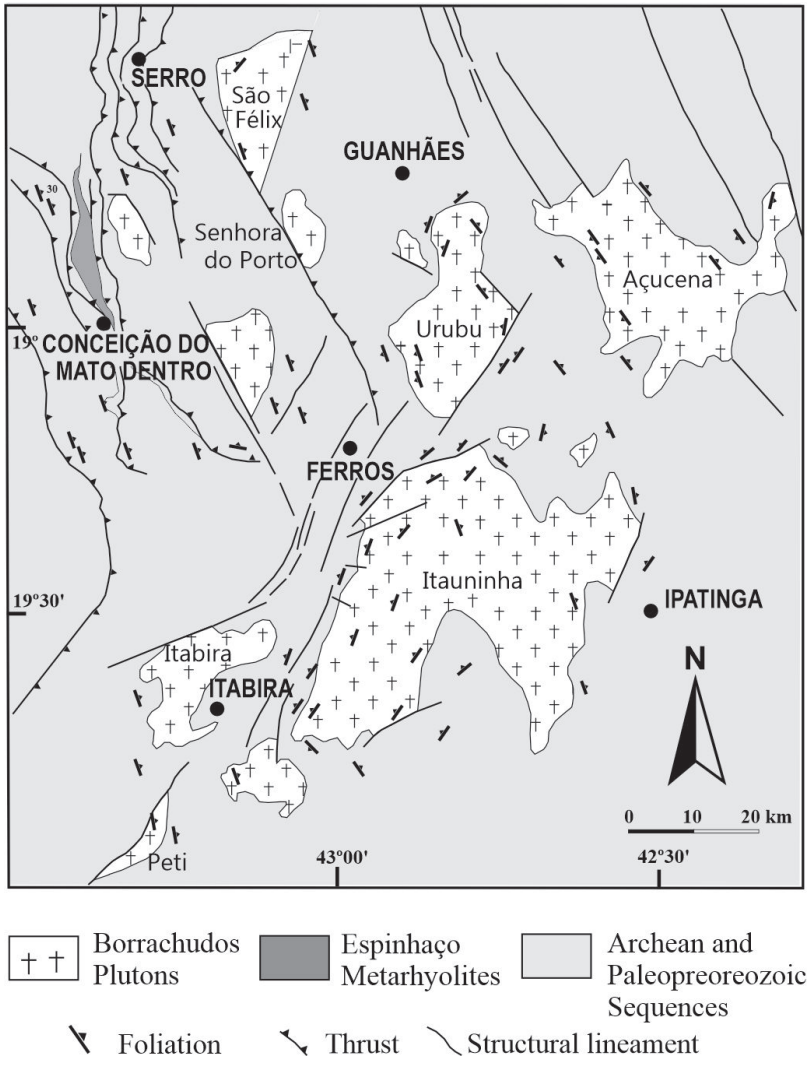

Figure 2. BGS plutons hosted in gneissic basement and Espinhaço metarhyolites in the southeastern Espinhaço Range (modified from Dussin 1994a).

The Brasiliano Cycle, which caused intense deformation and metamorphism linked with the development of thrust faults and emplacement of nappes in the fold belt, only weakly affected the plutons. Substantial shearing that can be seen in some places, on the western margins of the São Felix and Itauninha plutons, is probably related to reactivation of the major fracturation zones during the orogeny. The main effects of metamorphism within the plutons are the sericitization of feldspar and breakdown of biotite to chlorite (Dussin 1994b).

Geochronology

The granites of the BGS were previously considered to be genetically related to and deformed during an older orogeny of possible 2.2-1.9 Ga Transamazonian age (Grossi-Sad et al. 1990), but the ages of the plutons were not well known until recently. New geochronological data on the suite invalidates this hypothesis.

The available geochronological data for the plutons are summarized in Table I. Preliminary Rb-Sr whole-rock studies have yielded a wide scatter of points giving errochrons or poor isochrons (Teixeira et al. 1990). K-Ar biotite ages

Table I. A summary of available geochronological data for the BGS. Data according to [1] Teixeira et al. (1990), [2] Dussin (1994b), [3] Dussin (1994a), [4] Chemale Jr. et al. (1998), [5] Chaves et al. (2024).

Pluton	Rb-Sr (Ma)	K-Ar (Ma)	Pb-Pb (Ma)	U-Pb (Ma)
São Félix pluton	1426 ± 14 [1]	482.0 ± 5.8 (biotite) [2]	1729 ± 12 [3]	-
Urubu pluton	2140 ± 177 [1]	485.8 ± 7.6 (biotite) [2]	-	-
Itauninha pluton	-	475.4 ± 6.4 (biotite) [2]	~1600 [3]	-
Itabira pluton	-	-	-	1670 ± 32 [4]
Itauninha pegmatite	-	-	-	1675 ± 9 [5]

of ca. 480 Ma in the orthogneisses record to late-Brasiliano resetting (Dussin 1994b). Zircon Pb step-wise evaporation study yields ages for the emplacement of two plutons, the São Felix pluton being dated at 1729 ± 12 Ma and the Itauninha pluton at ca. 1600 Ma (Dussin 1994a, b). U-Pb analyze obtained in zircon of the Itabira pluton showed a 1670 ± 32 Ma (Chemale Jr. et al. 1998). A recent U-Pb LA-ICPMS dating in pegmatite zircons hosted in the Itauninha pluton presented a robust age in 1675 ± 9 Ma, confirming the previous age (Chaves et al. 2024).

These results show that emplacement of the plutons was coeval with the extrusion of the acid volcanics rocks related to the sedimentary sequences toward west in the Espinhaço Range. The principal and best known occurrence is to the north of Conceição do Mato Dentro town, where the age of the acid metavolcanics has been known for a long time. U-Pb dating of zircons from metarhyolites by Brito-Neves et al. (1979) indicated an age of 1770 Ma, and Machado et al. (1989) obtained U-Pb ages of 1711 ± 8 Ma and 1715 ± 2 Ma for the same sequence.

RESULTS

Petrography

The granites and especially the metarhyolites are weathered and exposures generally limited and discontinuous. This, combined with poor access, precludes systematic observation of the suite that could provide detailed information on granite zoning and/or a volcanic sequence. Nevertheless, our petrographic studies show that the Borrachudos granites are very homogeneous and there are no main petrographic features distinguishing different plutons.

The metarhyolites are also homogeneous and their mineralogical composition is essentially similar to that of granites. Modal compositions for granites and metarhyolites are plotted on QAP diagrams (Fig. 3); the range in composition of granites is limited to the alkali-feldspar granite and granite fields. The metarhyolites have similar composition, plotting within the alkali-feldspar rhyolite and rhyolite fields, certain samples showing a more alkaline trend.

Contrasting features in granites and metarhyolites are related to deformation and obviously magmatic structures; these last rocks within the fold belt also suffered mylonitization. Arrays of intrafolial folds, a conspicuous mylonitic foliation and an east-plunging stretching lineation are well developed. The main metamorphic affects are sericitization of feldspar and chloritization of biotite. Minor variations in texture and accessory mineral paragenesis are reflected in chemical differences, particularly the trace element composition.

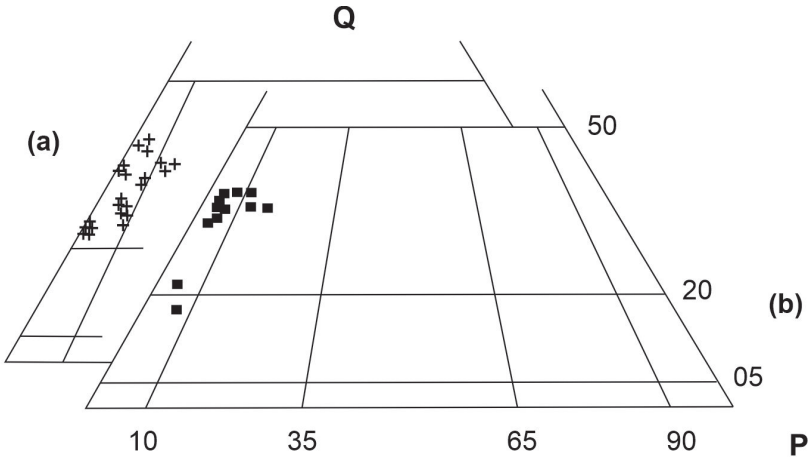

Figure 3. Classification and nomenclature to BGS (a) and Espinhaço metarhyolites (b), according to their modal mineral contents using the QAP diagram (based on Streckeisen 1976). Q = quartz, A = alkali feldspar, P = plagioclase.

Granites (and related pegmatites)

Most of the granites are medium-grained and, locally, porphyritic. They consist essentially of perthitic alkali feldspar and quartz, with biotite and minor hornblende. The perthite is generally inclusion-poor, with rare or no albite. The granites can be classified as hypersolvus to subsolvus granites. The perthite commonly consists of intergrowths of K-rich and Na-rich feldspar on microscopic or submicroscopic scale. The fine regular perthitic in intergrowths suggest unmixing of an originally homogeneous alkali-feldspar which were extracted from the residual liquids at temperature above the solvus. Coarse-grained perthites are less abundant and crystallized later. Quartz is present as large strained grains, small drop-like inclusions in mircrophertite or as symplectic intergrowths with feldspar.

Textual relations indicate that alkali-feldspar crystallized after plagioclase and generally, quartz. Deep brown biotite, the chief mafic mineral, and amphibole with characteristic green to brown pleochroism, crystallized after feldspar, quartz and most of the accessory phases characterizing agpaitic textures. These minerals are sub- to anhedral and intertitial to the felsic minerals. Biotite also fills fractures in the quartz and feldspar.

Accessory phases include fluorite, zircon, apatite, allanite, Fe-Ti oxides and molybdenite. Fluorite is a typical late-magmatic phase. Zircon appears most commonly as euhedral crystals, showing no optically detectable relict cores, associated with biotite and amphibole and may form the centers of pleochroic haloes in the host mineral. A morphologic study of zircon (Dussin 1994a) indicated that most of the crystals have predominantly the prism {100} with secondary prisms {101}. According to the classification of Pupin (1980), this morphology characterizes hypersolvus granites with crystallization temperatures about 850° C. The oxides constitute a series in which magnetite is abundant, and ilmenite appears as lattice-type intergrowths.

Pegmatites spatially related to BGS are abundant in the region between Santa Maria de Itabira and Ferros, in the so-called Santa Maria de Itabira Pegmatite District, which is part of the Eastern Brazilian Pegmatite Province – PPOB (Netto et al. 1998). These deposits occur in the interior or close to the Itauninha and Itabira plutons, intruded in archean gneisses, generally forming thin bodies less than 5 meters thick. There was always a question whether they were derived from the BGS, or else from possible sub-outcropping granitic intrusions of Brasiliano age, after all never really detected. In a way, this

presumption supported the maintenance of the pegmatitic district within the PPOB.

However, according to Chaves et al. (2024), new U-Pb analyzes (LA-ICPMS) on zircons from a pegmatite from the same district (Ponte da Raiz) showed a robust concordia-age at 1675 ± 9 Ma, indicating a crystallization age compatible with the BGS anorogenic magmatism. This pegmatite is the best studied of the entire district (Cassedanne et al. 1995), showing clear zoning, with a quartz core surrounded by microcline zone with small albitic replacement pockets. The typical mineralogy presents industrial beryl and aquamarine, as well as topaz, amazonite, monazite-(Ce), apatite, fluorite and columbite.

Although the emerald and alexandrite mineralizations also present in the region are attributed to hydrothermal processes derived from regional metamorphism (Jordt-Evangelista et al. 2016), the confirmation of pegmatogenesis associated with Borrachudos magmatism opens up an extensive field for new mineral research. According to London's (2008) classification, such pegmatites belong to the NYF "family" (niobium-yttrium-fluorine), and are rich in the last element precisely to mineralize the host rocks.

Acid volcanic rocks (metarhyolites)

The acid volcanic rocks generally contain quartz, microline, albite and minor biotite and magnetite. Microcline and quartz are the major mineral phases in metarhyolites, both as phenocrysts and as matrix constituents. The alkali-felspar megacrysts are euhedral, with a common albite rim. Phenocrysts of quartz, a few millimeters across, have bypiramidal habit and are commonly fractured and corroded. The matrix is holocrystalline and no vitroclastic structure was observed. It is composed mainly of microcrysts of K-feldspar and quartz, with minor plagioclase. Biotite, the only mafic silicate present, is less abundant than in the granites. It has generally recrystallized to chlorite forming mixed layers in which titanium and iron are present as grains of magnetite and leucoxene. Primary magnetite, more abundant than in granites, is usually disseminated as euhedral crystals or grains, in places with ilmenite intergrowths. Recognizable accessory phases are essentially fluorite, zircon and allanite. The morphological study of zircons indicated the same evolutionary trend as for the granites and crystallization temperatures about 850 °C (Dussin 1994a).

Mineral Chemistry

Alkali feldspar, amphibole, mica and Fe-Ti oxides have been analysed for major elements and F, using a CAMEBAX automated electron microprobe operated at 12 Kv and 1.5 µA beam current, at BRGM (Orléans, France). Complete analytical results and structural formulae of the mineral are given in Dussin (1994b).

Feldspars and amphiboles

The alkali feldspars constitute a low-temperature series with perthitic texture. This nature of the feldspar imposes the necessity for great care in microprobe analysis and interpretation of the results. Coarse-grained perthites, the most abundant textural types, have been analysed preferentially, the two phases being analyzed separately (Fig. 4). The K-rich phases, Or_{90-97} in granites and Or_{91-99} in metarhyolites, are always anorthite-depleted. Albite contents can reach 8 wt%. The Na-rich phase is chemically low albite, ranging from Ab_{96-100}, with less than 3% anorthite in rhyolites and 9% in granites, and is always orthoclase-poor, with contents less than 5% in rhyolites and 2% in granites. Alkali-feldspar textures indicate crystallization of homogeneous feldspar.

Temperatures above the solvus are required for extracting these crystals from the residual liquids (about 720°C at 5 kb water

pressure, according to Martin 1988). Unmixing of originally homogeneous crystals into K-rich and Na-rich phases indicates that the feldspar has been re-equilibrated during cooling and/or metamorphism, precluding the use of chemical data as constraints for determining temperatures of crystallization.

Hornblende is the amphibole primary phase in granites throughout the massif. It is Ca-rich and Ti-poor with enough Fe to cause dark brown-greenish pleochroism in thin sections. A-site occupancy is remarkably constant at about 0.30 to 0.40. Following the classification of Leake (1978), the amphibole ranges from Fe-hornblende to lightly Fe-tschermakitic hornblende (Fig. 5). The Mg ratio (Mg/Mg + Fe) evolves parallel to the biotite trend and decreases with increasing differentiation. The mineral compositions follow a trend similar to that of rock differentiation, with major substitution $Ca + Al^{(IV)} \Leftrightarrow Si + Na + K$ (Giret et al. 1980). Amphibole compositional evolution is represented in the Fig. 6. The crystals show a general trend of increasing F, Mg and Fe from center to edge, suggesting slightly oxidizing crystallization conditions. Weak compositional zoning, with Ti-enriched cores, seems related to late magmatic processes.

Biotite and Fe-Ti oxides

Main mica from the BGS is biotite with high Fe/(Fe + Mg) and low Al and Ti. Zoning of F, with outer parts of crystals enriched relatively to the

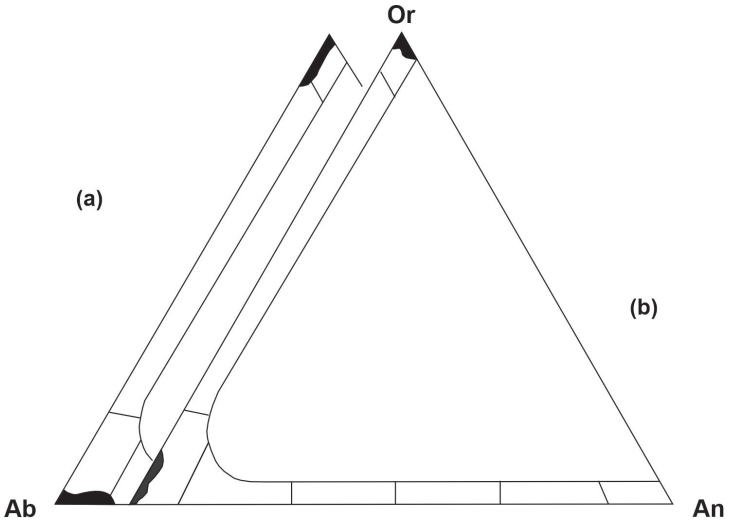

Figure 4. Solid solution in low-temperature feldspars from BGS and Espinhaço metarhyolites, showing compositional ranges of the microcline – low albite series.

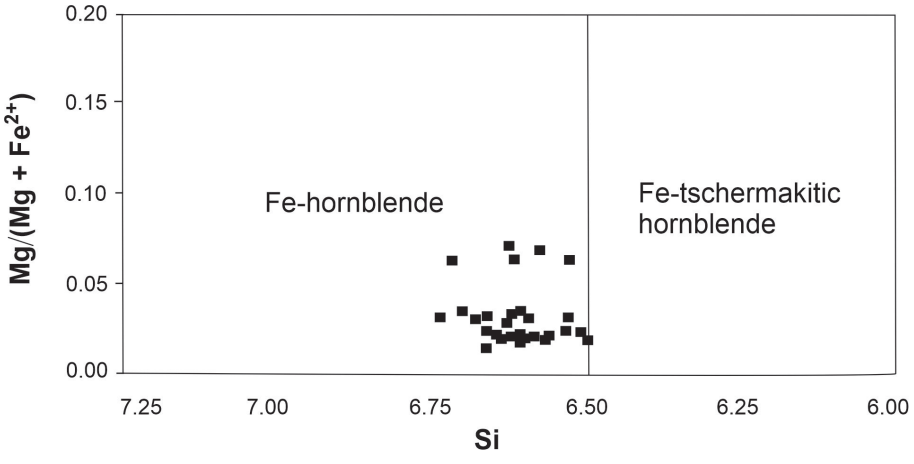

Figure 5. Classification of calcic amphiboles with $(Na + K)_A$ and Ti <0.50 (after Leake 1978).

centers, is also present. Biotite compositions are plotted on an M^{2+} – Al – Si triangular diagram (Fig. 7). The biotite from granites and rhyolites lie below the annite or phlogopite-muscovite line, and have similar low Al contents. Biotite of the rhyolites plot away from the line, showing a relative decrease in M^{2+} and slight enrichment in Si with contents about 2.9 in the structural formulae. This Si-enrichment can be related to that substitution scheme Mg + $2Al^{(IV)}$ ⇔ 2Si + vacant site, as previously described for metasomatic phlogopites (Seifert & Schreyer 1971).

The chemistry of the biotite reflects the composition of the host rocks. They plot in a narrow range of compositions, consistent with the marked uniformity of the suite. The restricted compositional variations are related to the differentiation of the rock and evolve towards the more differentiated terms. The low Al contents in biotite reflect the low magmatic concentration

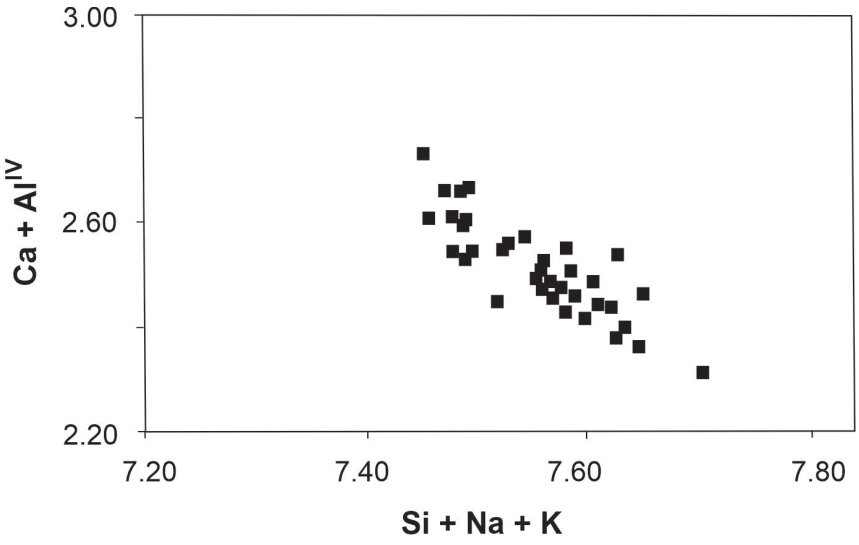

Figure 6. Amphibole compositional evolution expressed as a function of Ca + $Al^{(IV)}$ versus Si + Na + K.

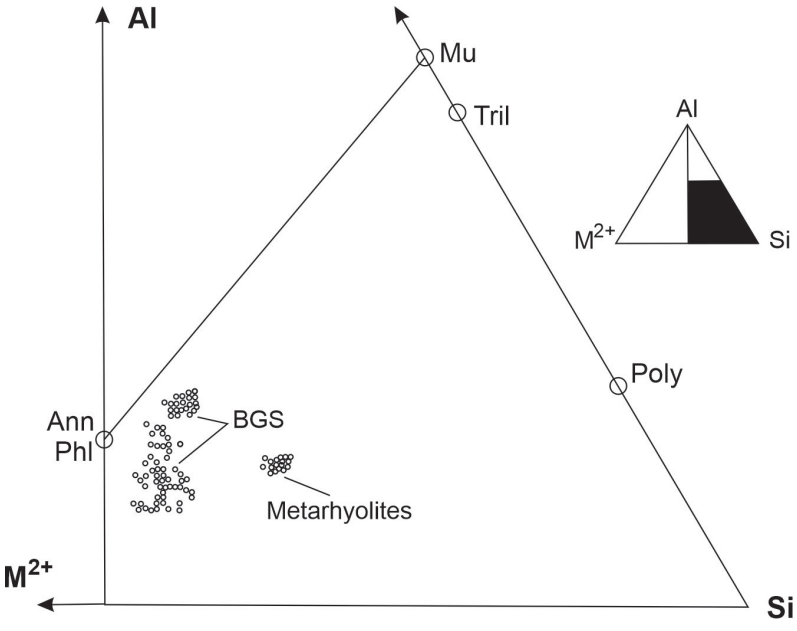

Figure 7. Plot of the compositions of ferromagnesian micas from Borrachudos granites and rhyolites on an M^{2+}-Al-Si diagram. Data are corrected for TiO_2 according to Robert & Maury (1979). End-members are annite (Ann), phlogopite (Phl), muscovite (Mu), trilithionite (Tril) and polylithionite (Poly).

of the element after the crystallization of alkali feldspar.

The first biotite crystallizes with the last feldspars and are, in general, more aluminous and magnesian than those of late crystallization. Furthermore, low $Al^{(IV)}$ contents associated with low Ti indicate low temperatures of mica extraction, in accordance with crystallization in the late magmatic stage (Robert 1976a, b). Reequilibration involving substitution of chiefly Fe^{+3} and Ti is common in the analyzed samples and is related to late magmatic and/or metamorphic effects. These processes generally produce an increase in Fe / (Fe + Mg) and a decrease in Ti towards the crystal margins, except in the rhyolites where no clear tendency can be detected.

The Fe-Ti oxide mineralogy in the Borrachudos granites and rhyolites constitutes a magnetite series. These minerals crystallized, in general, after the feldspar and quartz, but are enclosed in the hydrous silicates. Their present composition is 70-80% Fe_3O_4, a common consequence of subsolidus chemical re-equilibration in plutonic rocks (Lindsley 1976) and precludes any thermobarometric interpretation. On the other hand, the oxide component of the suite is significant and indicates a low level of oxygen fugacity during crystallization.

Geochemistry

Methodology

Chemical analyses were performed at the Centre de Recherches Petrographiques et Géochimiques (CRPG), Nancy, France, and at Geologia e Sondagens Ltda (GEOSOL), Belo Horizonte (Brazil). For the samples analyzed in GEOSOL, major and trace elements were analyzed by X-ray fluorescence, except the REE, which were analyzed using inductively coupled plasma (ICP) atomic emission spectrometry. At CRPG, all major and trace elements were analyzed by ICP. Analytical uncertainties are less than 5 to 10% for major elements, less than 10% for trace elements and about 5% for REE, except for contents to 1 ppm where uncertainly is about 15%.

Nd isotopic analyses were performed at the CNRS "Magmas et Volcans" laboratory (URA 10) at Clermont Ferrand, on a VG.54E mass spectrometer. The Nd isotopic composition was measured with a standard error of 0.000015 at 95% confidence level. Sm and Nd concentrations were measured by isotopic dilution with a mixed ^{149}Sm-^{150}Nd spike. The precision on the $^{147}Sm/^{144}Nd$ ratio is 0.2%.

While the granites show limited evidence of deformation or metamorphic recrystallization, the volcanic rocks, have been more strongly affected, with the development of thrusts and folds and pervasive metamorphic recrystallization. This, and the poor and discontinuous exposure, precluded systematic sampling of the suite. Altered or highly deformed rocks were not sampled. It is difficult, however, to be certain to what extent the chemical composition of the rocks may have been modified. The most obvious changes are related to the mobility of the alkalis, Sr and Ba. The REE content of the rocks is little or not at all affected by secondary alteration. The generally smooth REE pattern, with no suspicious anomalies, supports the assumption that the REE contents closely represent the magmatic concentrations. The Sm-Nd isotope system is little affected by secondary alteration (Faure 1986) while the Rb-Sr system, however, must be used with caution. Chemical analytical results are given in Tables II, III, IV and V.

Table II. Chemical analytical data for major, minor and trace elements of representative granite samples from BGS. Other authors data according to [1] Grossi-Sad et al. (1990), [2] Chemale Jr. et al. (1998), [3] Herz (1970), [4] Kanig (1985). (n) = Number of samples as plotting on Fig. 3. *All Fe as FeO. - No analyzed. n.d. = No detected.

Pluton	São Félix				S. do Porto		Urubu						Açucena				Itauninha-Itabira			Peti
Sample	SF.90	SF.45	SF.52	SF.[1]	SP.101	SP.97	U.35	U.36	U.48	U.87	U.97	U.6	A.69	A.211	A.111	A.220	IT.106	IT.[1]	IB.1	Pe. 1
(n)	1	2	3	-	4	4	6	7	8	9	10	11	12	13	14	15	16	-	[1,2,3]	[2,3,4]
SiO_2 %	72.54	72.70	76.45	74.50	74.50	76.20	69.00	70.50	70.10	70.90	71.93	72.20	67.80	71.30	74.05	75.10	71.50	74.30	74.26	75.07
TiO_2	0.16	0.29	0.13	0.21	0.21	0.20	0.58	0.43	0.47	0.46	0.36	0.43	0.62	0.30	0.21	0.17	0.35	0.21	0.23	0.24
Al_2O_3	13.27	12.60	12.17	11.70	11.70	11.40	12.10	13.20	13.50	13.70	13.73	12.80	12.40	12.60	11.70	11.20	13.00	12.20	11.45	12.43
FeO*	2.22	3.22	2.02	1.94	1.94	1.93	5.20	4.41	4.54	4.88	3.69	3.91	7.01	3.06	0.94	2.00	4.00	2.38	3.31	1.89
MnO	0.02	0.05	0.00	0.02	0.02	0.02	0.08	0.07	0.05	0.07	0.05	0.04	0.14	0.05	0.02	0.05	0.05	0.03	0.03	0.03
MgO	0.00	0.08	0.03	0.04	0.04	0.13	0.29	0.24	0.22	0.18	0.12	0.40	0.40	0.06	0.04	0.04	0.28	0.25	0.10	0.06
CaO	0.92	0.98	0.70	0.82	0.82	0.67	1.80	1.50	1.60	1.60	1.10	1.50	2.10	1.10	0.85	0.72	1.30	0.96	0.89	0.75
Na_2O	2.93	2.50	3.10	2.90	2.90	3.10	4.20	4.10	4.00	3.00	3.07	3.10	3.90	4.20	2.90	3.60	4.10	3.20	3.55	3.23
K_2O	6.64	6.40	5.18	6.30	6.30	5.20	5.40	4.60	4.80	4.30	5.42	4.60	4.20	5.70	6.30	5.60	4.70	5.80	5.37	5.02
P_2O_5	0.03	n.d.	0.02	0.14	0.14	0.18	0.12	0.06	0.09	0.08	0.06	0.11	0.15	n.d.	n.d.	n.d.	n.d.	0.05	0.06	0.01
F	-	0	-	0.27	0.27	0.25	0.07	0.03	0.07	0.09	-	0.17	0.16	0.12	0.27	0.12	0.06	0.28	0.26	0.60
PF	0.68	1.07	0.36	0.75	0.75	0.50	0.66	0.74	0.49	0.66	1.37	0.65	1.10	1.29	0.88	1.40	0.60	1.05	0.86	0.92
Total	99.4	100.0	100.2	100.0	100.0	100.00	99.5	99.9	99.9	99.9	100.9	99.9	100.0	99.8	98.2	100.0	99.95	100.7	100.4	100.2
Ba ppm	823.0	2240	229.0	160.0	740.0	260.0	1150	1180	1160	1020	1419	940.0	640.0	950.0	160.0	360.0	1200	840.0	360.0	522.0
Rb	265.0	170.0	242.0	360.0	160.0	400.0	140.0	150.0	190.0	200.0	141.0	250.0	230.0	190.0	360.0	280.0	160.0	230.0	289.0	295.0
Sr	54.2	160.0	31.6	35.0	140.0	30.0	150.0	140.0	150.0	120.0	120.0	140.0	60.0	93.0	35.0	51.0	140.0	120.0	32.0	40.0
V	0.5	-	1.2	-	61.0	-	102.0	66.0	-	-	2.2	80.0	56.0	-	-	-	-	-	-	-
Zr	270.0	580.0	218.0	220.0	400.0	280.0	880.0	660.0	620.0	780.0	415.0	520.0	960.0	410.0	220.0	270.0	520.0	-	500.0	334.0
Cr	10.3	-	3.8	-	-	-	-	-	-	-	1.8	-	-	-	-	-	-	-	-	-
Co	0.5	n.d.	0.6		n.d.	-	n.d.	n.d.	-	-	1.5	6.0	n.d.	-	-	-	-	-	-	-
Ni	4.6	-	6.9	-	-	-	-	-	-	-	1.1	-	-	-	-	-	-	-	12.0	15.5
Cu	6.6	14.0	2.3	2.0	n.d.	6.0	3.0	4.0	4.0	3.0	7.3	5.0	6.0	4.0	2.0	n.d.	7.0	3.0	21.5	20.0
Zn	82.4	99.0	46.1	160.0	62.0	67.0	157.0	109.0	121.0	164.0	78.2	106.0	196.0	75.0	160.0	86.0	147.0	89.0	130.0	124.5
Ga	29.3	35.0	24.5	21.0	20.0	20.0	24.0	23.0	26.0	24.0	25.1	24.0	30.0	19.0	21.0	18.0	25.0	20.0	30.0	23.0
Sc	2.3	9.0	2.0	-	n.d.	-	10.0	7.0			3.9	18.0	18.0		-			-	72.0	-
Nb	22.6	54.0	19.5	50.0	36.0	48.0	36.0	26.0	26.0	44.0	22.3	20.0	57.0	62.0	50.0	28.0	26.0	28.0	134.0	50.0
Y	113.0	240.0	80.5	72.0	23.0	49.0	78.0	52.0	42.0	94.0	34.3	112.0	120.0	92.0	72.0	22.0	28.0	140.0	25.5	165.0
Th	37.0	-	45.9	-	-	-	-	-	-	-	8.2	-	-	-	-	-	-	-	5.0	-
Be	6.0	2.0	5.4	8.0	7.0	8.0	3.0	n.d.	2.0	3.0	1.6	2.0	3.0	3.0	8.0	2.0	n.d.	2.0	72.0	7.0
U	8.0	-	6.7	-	-	-	-	-	-	-	1.0	-	-	-	-	-	-	-	-	-
Ta	2.6	-	1.5	-	-	-	-	-	-	-	1.3	-	-	-	-	-	-	-	-	-
Hf	11.0	-	10.1	-	-	-	-	-	-	-	12.4	-	-	-	-	-	-	-	-	-

Table III. Chemical analytical data for major, minor, and trace elements of representative Espinhaço metarhyolite samples. Same informations as Table II.

Samples	ER.3A	ER.3B	ER.14A	ER.14B	ER.14C	ER.16	ER.116E	ER.116F	ER.118	Pt. [1]	Rg.[2]	Hg.[3]	Uh.[4]
(n)	17	18	19	20	21	22	23	24	25		{5}	{5}	{6}
SiO2 %	72,20	72,25	76,43	74,70	75,39	67,59	72,07	75,55	71,34	76,57	74,07	69,13	65,08
TiO2	0,13	0,20	0,29	0,22	0,22	0,56	0,53	0,19	0,64	0,31	0,28	0,47	0,70
Al2O3	13,34	13,86	11,89	11,42	11,57	12,50	11,83	11,28	12,05	12,46	12,41	12,41	14,12
FeO*	1,10	3,51	0,83	3,16	3,33	6,69	4,40	2,66	6,08	2,69	3,31	5,54	5,86
MnO	0,02	0,04	-	0,07	0,07	0,14	Traces	0,03	0,10	0,06	-	-	0,66
MgO	0,08	0,13	Traces	0,08	0,08	0,30	0,32	0,11	0,55	0,24	-	0,10	0,35
CaO	2,26	0,40	0,83	0,46	0,39	1,77	1,54	0,83	0,54	1,17	0,58	0,34	1,69
Na2O	2,78	2,78	3,47	2,82	3,12	4,19	2,83	2,11	3,45	3,68	2,96	1,31	3,29
K2O	4,45	4,80	5,27	5,35	5,00	4,50	4,50	5,91	4,09	3,44	5,17	3,44	6,62
P2O5	0,02	Traces	0,02	0,03	0,02	0,16	0,05	Traces	0,16	Traces	Traces	4,81	0,13
F	-	-	-	-	-	-	-	-	-	-	-	-	0,19
P.F.	1,75	1,65	0,73	0,76	0,52	1,21	1,73	1,00	0,58	-	-	0,12	1,23
Total	96,38	97,97	99,03	98,32	99,71	99,61	99,80	99,67	100,00	100,62	98,77	97,66	99,92
Ba ppm	250	-	165	118	111	658	202	427	1598	201	-	484,80	-
Rb	254	296	245	278	258	222	211	273	106	386	-	166,40	212
Sr	19	-	25	12	16	70	18	32	92	7	-	46,40	39
V	46	-	1	1	<5	6	10	n.d.	19	-	-	9,20	-
Zr	520	-	774	695	706	877	658	650	522	372	-	722,60	745
Cr	5	5	5	6	11	7	6	n.d.	n.d.	5	-	2,00	n.d.
Co	-	-	0	0	n.d.	n.d.	2	n.d.	5	-	-	-	-
Ni	7	13	3	3	8	8	5	5	n.d.	6	-	8,60	n.d.
Cu	-	-	5	3	12	18	6	16	8	-	-	-	-
Zn	-	-	68	81	55	204	97	52	77	-	-	-	-
Ga	-	-	32	37	36	30	33	31	18	-	-	-	-
Sc	-	-	2	2	2	9,8	5	1,5	7,4	-	-	-	-
Nb	-	-	122,0	109,0	101,0	87,0	109,0	122,0	23,0	-	-	-	148,32
Y	-	-	135,0	351,0	251,62	163,03	1685,0	1814,0	78,46	-	-	-	118,17
Th	-	-	46	47	48	38	45	41	16	-	-	-	-
Be	-	-	1	3	3,5	4	5	5,5	1,6	-	-	-	-
U	-	-	10,5	9,6	-	-	8,6	-	-	-	-	-	-
Ta	-	-	8,3	8,0	-	-	8,3	-	-	-	-	-	-
Hf	-	-	27,5	25,3	-	-	25,3	-	-	-	-	-	-

Table IV. Chemical analytical data for rare earth elements of representative granite samples from BGS. Same informations as Table II.

Pluton	São Félix				S. do Porto		Urubu						Açucena				Itauninha-Itabira			Peti
Sample	SF.90	SF.45	SF.52	SF.[1]	SP.101	SP.97	U.35	U.36	U.48	U.87	U.97	U.6	A.69	A.211	A.111	A.220	IT.106	IT.[1]	IB.1	Pe. 1
(n)	1	2	3	-	4	5	6	7	8	9	10	11	12	13	14	15	16	-	[1,2,3]	[2,3,4]
La ppm	151.9	43.4	85.7	156.8	740.0	147.8	49.3	118.0	100.5	48.3	49.0	139.5	162.8	156.8	156.8	90.3	22.9	214.6	132.5	82.5
Ce	2770	88.8	170.6	283.1	160.0	250.9	96.7	193.9	182.2	183.9	93.5	246.5	295.8	283.1	283.1	164.0	63.1	231.2	234.0	151.5
Nd	105.4	53.4	66.1	121.0	140.0	104.1	59.9	79.5	73.8	63.2	41.8	101.1	127.0	121.6	121.6	69.9	31.5	145.8	92.2	72.1
Sm	20.2	10.9	13.5	32.3	61.0	26.3	14.3	14.4	13.8	15.8	7.9	19.8	25.7	32.1	32.1	18.6	7.5	28.3	19.8	13.9
Eu	1.1	3.3	0.5	0.9	400.0	0.1	2.5	2.0	2.5	2.2	2.2	2.3	2.8	0.9	0.9	1.0	2.1	2.1	1.3	0.8
Gd	18.1	9.4	12.2	23.3	-	18.2	12.8	12.0	11.7	16.1	6.6	17.2	22.1	22.3	22.3	13.8	7.2	29.1	16.8	11.0
Dy	18.2	6.0	13.2	21.1	n.d.	17.1	12.6	10.4	9.9	17.1	6.5	16.8	21.3	21.0	21.0	12.1	7.1	28.0	15.7	10.0
Er	10.2	3.1	7.6	11.3	-	10.4	7.1	5.7	5.8	10.4	3.4	11.2	13.2	11.3	11.3	7.6	4.2	6.0	6.4	6.2
Yb	10.8	2.3	7.5	8.8	n.d.	9.4	5.9	4.6	5.1	9.0	3.6	10.7	11.3	8.8	8.8	6.0	3.9	15.5	8.4	6.5
Lu	1.4	0.3	1.0	1.0	62.0	1.1	0.7	0.5	0.6	1.1	0.5	1.3	1.4	1.0	1.0	0.8	0.5	1.8	0.9	0.8
(La/Yb)n	9.5	12.4	7.4	12.0	20.0	10.6	5.6	17.3	13.3	3.6	9.1	8.8	9.7	12.0	12.0	10.2	4.0	9.3	10.6	8.6
(La/Sm)n	4.7	2.5	4.0	3.1	n.d.	3.5	2.2	5.2	4.6	1.9	3.9	4.4	4.0	3.1	3.1	3.0	1.9	4.8	4.2	3.7
(Gd/Yb)n	1.4	3.3	1.3	2.1	36.0	1.6	1.7	2.1	1.8	1.4	1.5	1.3	1.6	2.0	2.0	1.9	1.5	1.5	1.6	1.4
Eu/Eu*	0.2	1.0	0.1	1.0	23.0	0.1	0.5	0.6	0.6	0.4	0.9	0.4	0.3	0.1	0.1	0.2	0.9	0.2	0.2	0.2

Table V. Chemical analytical data for rare earth elements of representative Espinhaço metarhyolite samples.

Samples	ER.3A	ER.3B	ER.14A	ER.14B	ER.14C	ER.16	ER.116E	ER.116F	ER.118
(n)	17	18	19	20	21	22	23	24	25
La	123,30	-	78,75	515,20	229,71	164,52	253,60	312,67	171,95
Ce	227,60	-	149,20	397,90	418,41	297,21	135,80	377,07	260,42
Nd	90,67	-	56,72	354,20	167,35	120,1	150,40	161,52	122,22
Sm	24,92	-	11,47	66,76	37,56	25,58	48,04	50,77	22,34
Eu	1,05	-	0,58	2,45	2,00	2,88	4,28	2,22	4,03
Gd	17,00	-	12,98	61,29	30,48	20,92	140,80	60,64	16,84
Dy	12,36	-	20,60	59,77	32,38	21,79	279,40	96,25	14,18
Er	7,05	-	13,46	31,15	17,14	11,2	165,50	92,58	6,56
Yb	7,75	-	13,76	26,43	17,6	12,12	90,75	130,03	6,55
Lu	1,10	-	2,08	3,93	2,53	1,87	12,68	21,55	0,94
(La/Yb)n	10,74	-	3,86	13,16	8,81	9,16	1,89	1,62	17,72
(La/Sm)n	3,12	-	4,32	4,86	3,85	4,05	3,32	3,88	4,85
(Gd/Yb)n	1,77	-	0,76	1,87	1,40	1,39	1,25	0,38	2,08
Eu/Eu*	0,15	-	0,14	0,12	0,18	0,37	0,15	0,12	0,61

Major elements

The granites and rhyolites are homogeneous in chemical composition. With regard to the Shand parameters, most of the analyses plot in the metaluminous to subalkaline fields (Fig. 8). The presence of points representative of rhyolites in the peraluminous field is due to the loss of K_2O + Na_2O in the tectonized volcanics, with a resulting increase in the Al/alkali ratio. The presence of annite, Fe-hornblende and plagioclase with lower Na contents in granites is reflected in their chemical composition. In accordance with the observed mineralogical composition of the rocks, they have characteristically high K_2O/Na_2O ratios and K_2O, high FeO/FeO + MgO and low CaO and Al_2O_3 contents. F contents range from 0.03 to 0.60 wt%. Scatter of the K_2O and Na_2O contents confirms the secondary remobilization of these constituents. All these features are characteristic of A-type within-plate granites (Loiselle & Wones 1979).

Trace elements

Compatible trace elements Cr, Ni and Cu are low in granites and metarhyolites, and highly charged elements, particularly Rb, Zr, Nb, REE and Zn are enriched. High Ga/Al ratios are ubiquitous in the massif (Fig. 9). Geochemical patterns of these rocks normalized to ocean ridge granites show a general decrease in abundances from Rb to Yb. The high values of K_2O, Rb and Th are characteristic. The range of values from Zr to Yb has roughly flat distributions with the average close to the normalization values. The range of geochemical patterns of the suite and well known within-plate granites of different geological settings are compared (Fig. 10).

A significant distinctive feature of the Espinhaço sequence, when compared to oceanic island and rift granites, is enrichment in Rb and Yh. Such selective enrichment and the characteristic features of the BGS as a whole, suggest crustal involvement in the genesis of the magma, a hypothesis that is consistent with the isotopic data. In accordance with these interpretations, the trace element discriminant diagrams, Nb-Y and Rb-Nb + Y also indicate magma formation in within-plate settings (Fig. 11). The most significant feature of both diagrams is the complete separation of the collisional granites and the marked enrichments in Nb and Rb in relation to the mantle-dominated patterns of the oceanic ridge granites.

Rare Earth elements

The REE patterns of the granites from the BGS indicate close similarity among the plutons, in accordance with petrography and the chemistry of the major and other trace elements. They have high total REE and steep LREE patterns (Tables III and V, Figs. 12 and 13). The $(La/Yb)_N$ rates vary from 3.6 to 20.0; they all have large negative Eu anomalies (Eu/Eu* between 0.97 and 0.09). General distribution of the REE patterns is comparable to the typical ones of the subalkaline and metaluminous granitic rocks.

The analysis of the plutonic and volcanic patterns as a whole indicates that: (a) the LREE fractionation in granites is like that of the metarhyolites, with $(La/Sm)_N$ = 1.92 to 4.77 and 1.95 to 4.86, respectively; (b) the HREE patterns of the granites are characterized by a negative slope, steep between Yb and Lu, whereas the rhyolite patterns are slightly flatter or in some instances show a positive slope; (c) Ce is systematically enriched in the granites, a feature not present in the metarhyolites; (d) REE contents in the rhyolites are higher than in granites.

It is difficult to relate the individual differences in granites and metarhyolites to fractional crystallization, except the variations of the Eu anomaly associated with plagioclase fractionation. However, REE contents may be controlled by the crystallization of small

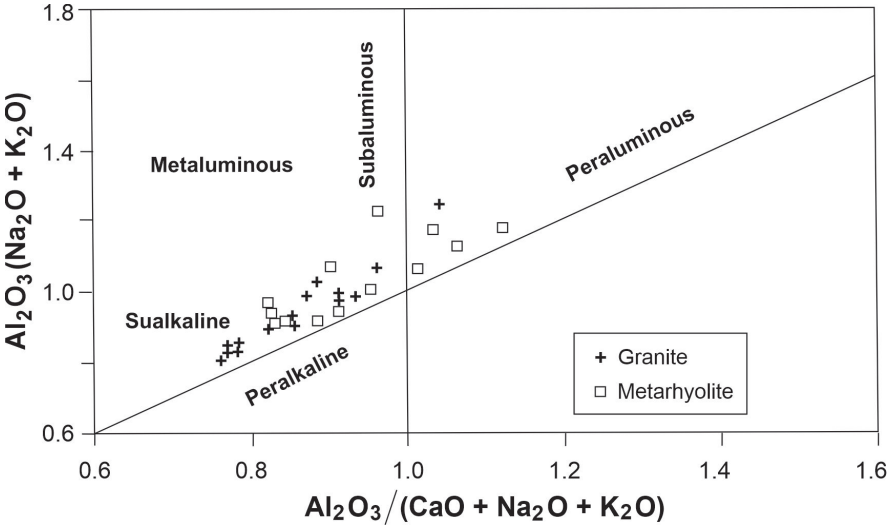

Figure 8. Alumina saturation diagram for Borrachudos granites and metarhyolites (after Maniar & Piccoli 1989). Crosses = granites, open circles = metarhyolites.

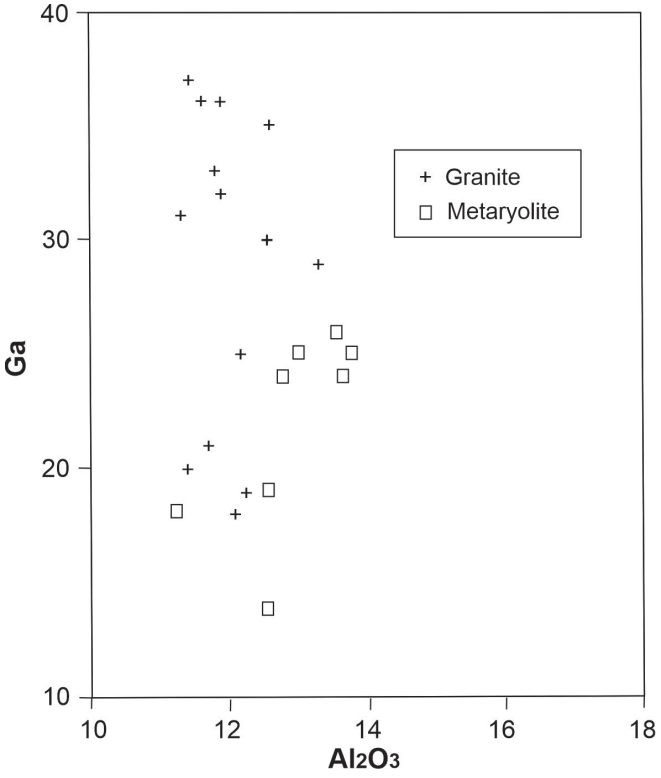

Figure 9. Plot of Ga versus Al_2O_3 to Borrachudos granites and Espinhaço metarhyolites.

amounts of accessory minerals. The enrichment in Ce observed systematically in granites may be a function of the abundance of allanite, monazite and possibly fluorine-bearing minerals, which are strongly Ce-selective. The HREE content is higher in zircons, and the role of this mineral is demonstrated by the high contents in both Zr and HREE in several samples, particularly in the metarhyolites.

Accompanying high Y contents in some instances suggest that xenotime may be also responsible for HREE enrichment (samples ER.116E and ER.116F). The REE contents of rhyolites, higher than those of granites, show no correlation with the rock differentiation indexes,

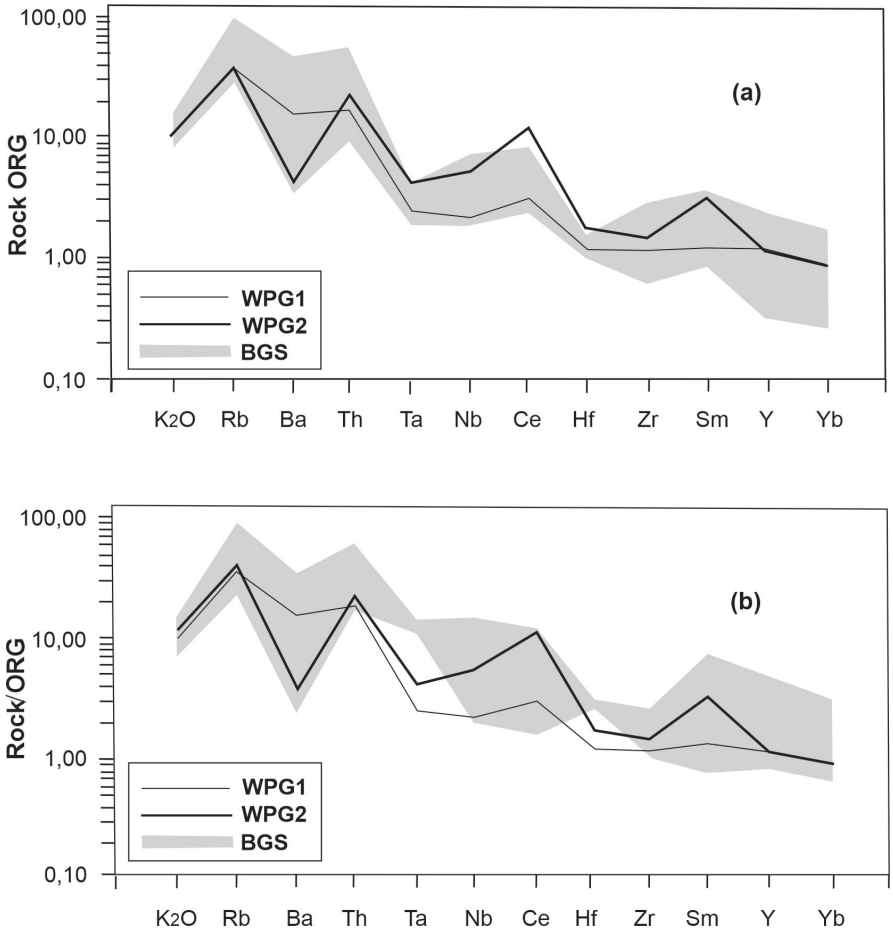

Figure 10. Ocean ridge granite normalized geochemical patterns for the range of the analyses, given in Tables II and III, of BGS granites (a) and metarhyolites (b). Values with a great discrepancy from the average have been unknown. Normalizing values and curves for comparison from Pearce et al. (1984). WPG_1 = within plate granites, WPG_2 = within plate granites with attenuated continental lithosphere.

indicating that this feature cannot be related to fractional crystallization. It seems possible that it is due to different rates of crustal assimilation during ascent of the granitic and rhyolitic magmas to the surface, but the possibility of later disturbances cannot be precluded.

Isotope Nd and Sr data

Six granites and rhyolites samples from the BGS have been analyzed for Sr and Nd isotopic compositions, Analytical results are listened in Table VI and shown in Figure 14, with the results of the analyses of geostandards and the physical constants used. The initial ∈nd values for granites and metarhyolites were back-calculated to 1730 Ma. The results vary within the range from -8.8 to -10.1 for granites and from -6.2 to -7.2 for metarhyolites. These results indicate that the Nd isotopic compositions are not as homogeneous as expected from the rather uniform petrographic and chemical features of the rocks.

The high negative values strongly suggest that a lower crustal source was involved in the formation of the magmas precluding a mantle-derived input. A possible explanation for heterogeneity of the data involves assimilation of different rates of crustal components by granites and rhyolites during pool in the crust or ascent of the magmas to the surface. This conclusion seems be supported by different contents of some trace elements and REE in granites and metarhyolites.

Sm-Nd model ages reflect the average amount of time that the constituents of the source have resided in the crust since derivation

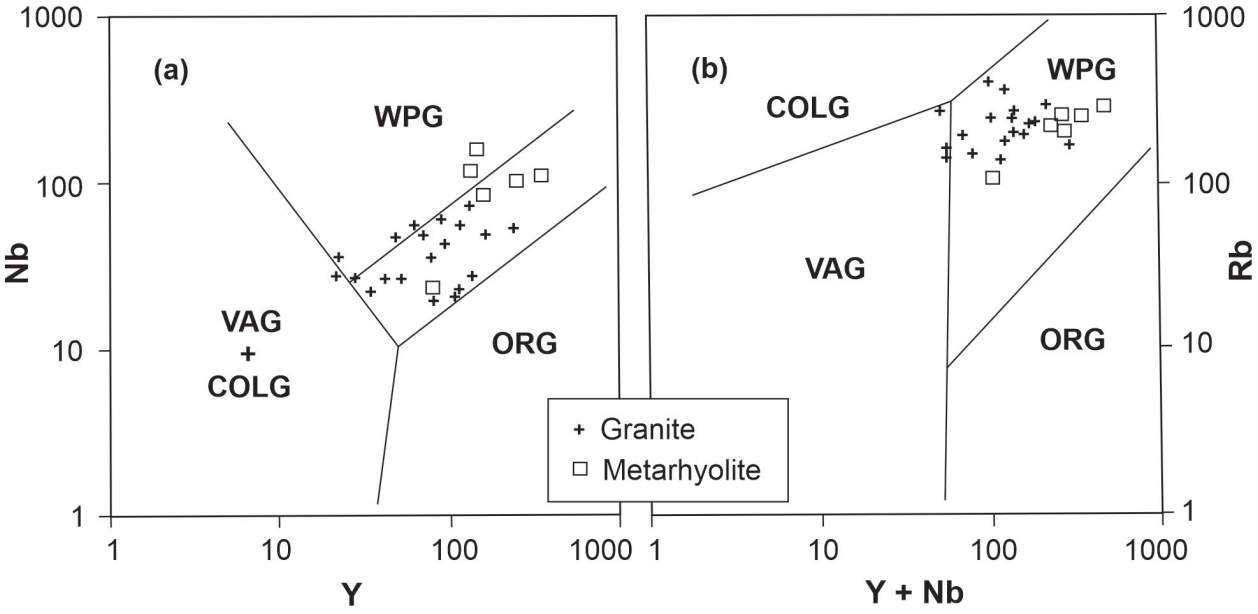

Figure 11. Borrachudos granites and Espinhaço metarhyolites data plotted on the Nb – Y and Rb – (Nb + Y) discrimination diagrams of Pearce et al. (1984). Fields of syn-collision (COLG), volcanic-arc (VAG), within plate (WPG) and ocean ridge (ORG) granites are indicated.

from a model mantle reservoir, assuming that the Sm-Nd ratio has not changed since derivation. The crustal residence ages have been calculated using the measured present-day values of $^{143}Nd/^{144}Nd$, assuming a depleted mantle reservoir (T_{DM}).

The analysed samples yielded T_{DM} ages ranging from 2.79 to 3.01 for granites and 2.57 to 2.85 for metarhyolites, suggesting derivation from Archean crust. Four analysed samples define a Rb-Sr whole rock regression line yielding an age of 1716 ± 105 Ma and an initial $^{87}Sr/^{86}Sr$ ratio of 0.7057 ± 0.0095 (Fig. 14). This age is interpreted as the time of emplacement of the suite and is supported by Pb-Pb single zircon age of 1729 ± 14 Ma (Dussin 1994a) and a U-Pb LA-ICPMS age also in zircon of 1675 ± 9 Ma (Chaves et al. 2024).

Two samples of metarhyolites plot underneath the isochrone indicating that these rocks were affected by post-magmatic disturbances. The initial $^{87}Sr/^{86}Sr$ ratio is surprisingly low, between 0.6695 and 0.7036 for granites. The single metarhyolite sample that plot on the isochrone yielded $^{87}Sr/^{86}Sr$ of 0.7224. If any petrogenetic information can be extracted of this data, as suggested by their coherent behavior in the isochronic diagram, it indicates that the Borrachudos magmas have been originated of partial fusion of a crustal source that is not very radiogenic and/or old as implied by range of T_{DM} ages. A Nd and Sr diagram illustring compositional features of the metarhyolites is depicted (Fig. 15).

PETROGENETIC DISCUSSIONS

Several petrogenetic schemes have been proposed for the origin of A-type suites in order to explain their major distinctive features, i.e, relatively dry, high-temperature, halogen-rich magmas and enrichment in highly-charged cations such as Nb, Zr, Y, Ga and REE. These models are of three types: (1) fractionation of a mantle-derived basaltic magma to yield alkali-rich differentiates (Loiselle & Wones 1979, Javoy

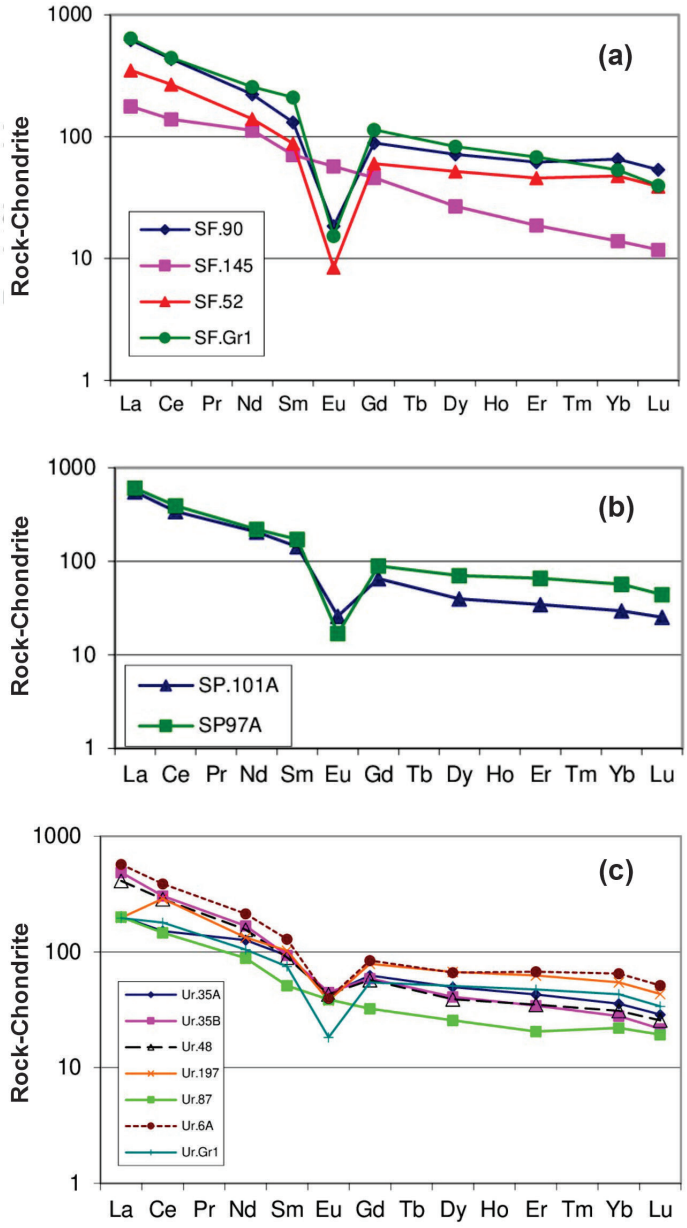

Figure 12. Chondrite-normalized REE patterns of the BGS. Analyses of granites from (a) São Félix, (b) Senhora do Porto, and (c) Urubu plutons (analytical data in Tables II and III; normalization values after Evensen et al. 1978).

& Weis 1987); (2) alkali and halogen metasomatic enrichment of a mafic magma (Currie et al. 1986, Taylor et al. 1980); and (3) high temperature partial melting of lower continental crust from which a granitic magma has already been extracted in an earlier event (Collins et al. 1982, Whalen et al. 1987, Anderson & Bender 1989).

For the BGS, the major obstacle to the first model is the absence of associated syenites. Mantle-derived magmas could have existed contemporaneously with the Borrachudos magma but there is no evidence of their coexistence. Kimberlites and lamproites are absent in the Espinhaço basin; the origin of diamonds in the region is related to intrusions inside the São Francisco craton (Chaves 1997, Chaves et al. 1998, 2001). In the metasomatic model, Taylor et al. (1980) suggested that the peralkaline character of anarogenic granites results from

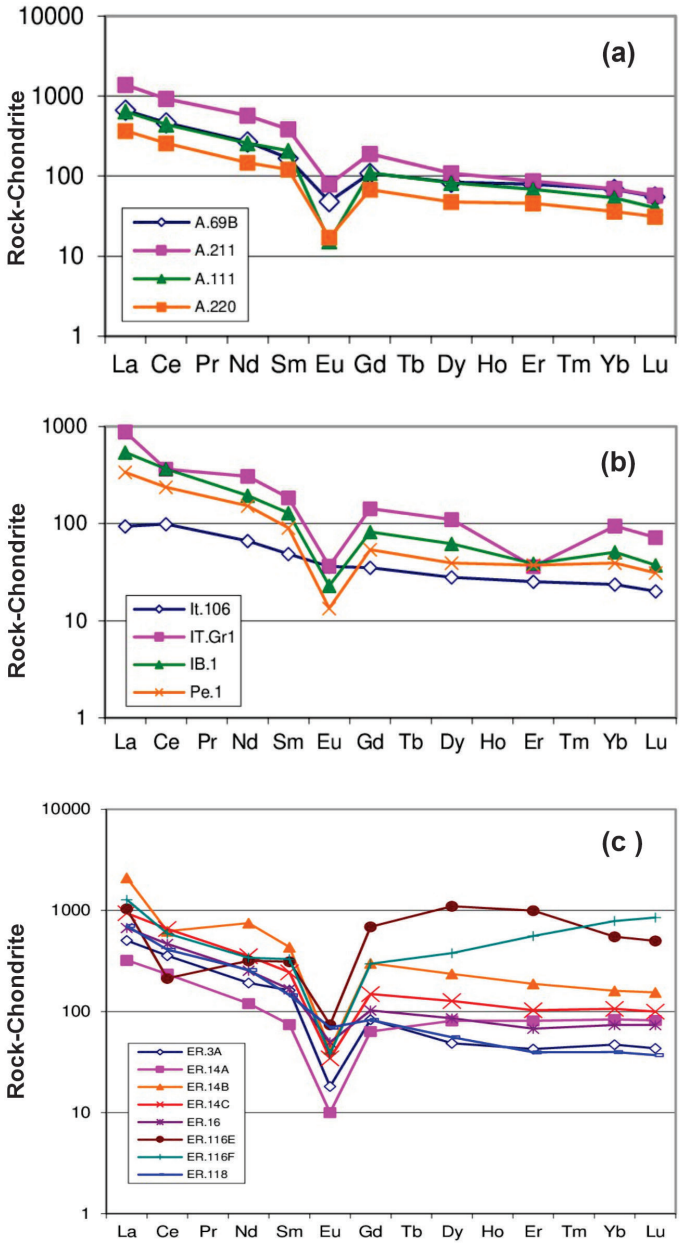

Figure 13. Chondrite-normalized REE patterns of the BGS. Analyses of granites from (a) Açucena, (b) Itauninha, Itabira and Peti plutons, and (c) metarhyolites (analytical data in Tables II and III; normalization values after Evensen et al. 1978).

metasomatism by a CO^{2-} and halogen-rich phase during and after emplacement.

However, the large-scale homogeneity in peralkaline magma is an argument against local and structurally controlled processes such as metasomatism (Whalen et al. 1987). In the third model, melting would involve fluid-absent breakdown of a residual source enriched in halogen-rich micas and amphiboles. Melting would have taken place in a fluid-present regime with volatiles other than H_2O, supplied from a subcrustal source (Clemens & Wall 1981). With respect to the refractory nature of the source, fusion would occur at high temperatures, and an extra-crustal heat source, such as a mantle-derived magma, would be required.

According to the scheme below, can be explained a majority of the most significative petrogenetic and geochemical features for the BGS and associated metarhyolites. The A-type

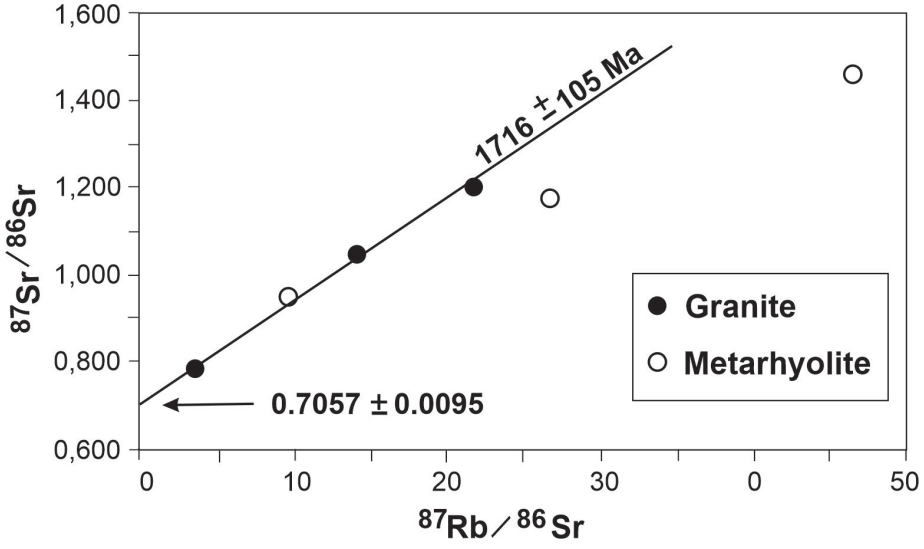

Figure 14. $^{87}Sr/^{86}Sr$ versus $^{87}Rb/^{86}Sr$ plots for BGS granites and Espinhaço metarhyolites. Solid circles = granites, open circles = metarhyolites.

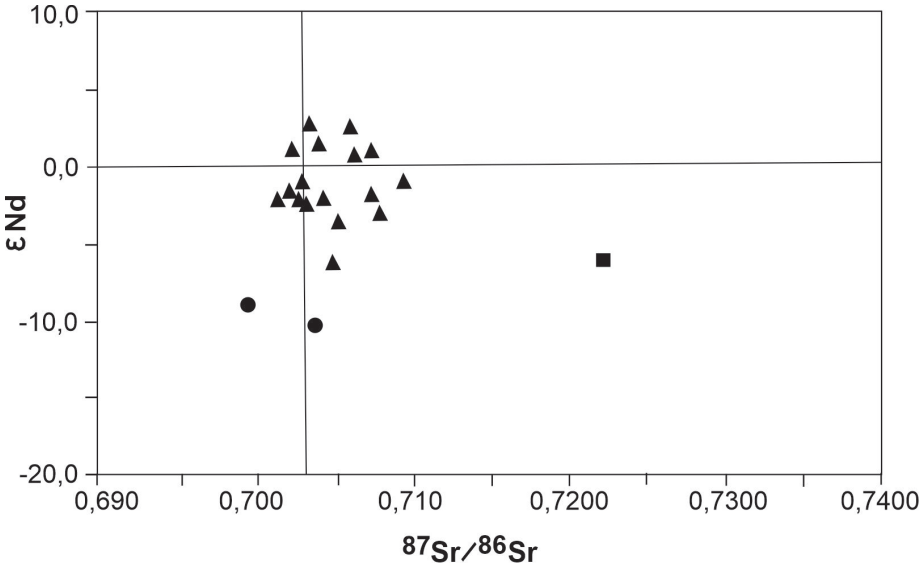

Figure 15. $\varepsilon Nd_{1730\ Ma}$ versus the initial $^{87}Sr/^{86}Sr$ ratio for the BGS. Data from about 1.5 Ga Proterozoic anorogenic granites from North America (after Anderson 1983, Anderson & Morrison 1992) are ploted for comparison. Solid circles = granites, solid square = metarhyolite, solid triangles = North American granites.

Borrachudos magma was emplaced at a rather shallow crustal level, probably at temperatures higher than 850° C. The magma was thus very hot for a granite or rhyolite, above the temperatures inferred for I- and S-type magmas with similar SiO_2 contents (Clemens & Wall 1981). However, the late crystallization of the amphibole and biotite in the granites indicates that the magma was relatively dry. Experimental data confirm this conclusion and show that biotite and alkali feldspar is function of the f_{H2O} in the magmas and that values less than 2 % are necessary for the observed sequence of crystallization (Maale & Wyllie 1975).

The major geochemical features for the BGS appear also to be consistent with this model:

(a) The high (Na + K)/Ca, Fe/Fe + Mg and low Al of the magmas could result from the breakdown of residual micas and the highly refractory nature of any residual calcic plagioclase and mafic phases;

(b) Thermodynamic data indicate that, for the necessary thermal stability of micas and amphiboles in the source, a Fluorine-rich

composition is required for these minerals (Holloway & Ford 1975 cited in Collins et al. 1982);

(c) The Ga enrichment relative to Al is explained by the preferential trapping of Al in the residual plagioclase;

(d) The contents of highly charged cations, Zr, Nb, REE and Zn are related to the halogen concentrations in the magma, particularly F, which distorts the aluminosilicate structure, providing sites for these cations and stabilizing metallic complexes (Collins et al. 1982);

(e) The highly negative ε_{Ndi} support the hypothesis of melting from a continental crustal source.

REGIONAL TECTONIC EVOLUTION

The requirement of the model for depleted protoliths in the lower crust is met by a magmatic event associated to the open of the basin that generated the Espinhaço sedimentary basin and metarhyolites at ca. 1.7 Ga, together with the BGS intrusions to east. Mantle diapirism or the emplacement of mantle-derived magmas in continental crust during this extensional tectonic, at the onset of the Mesoproterozoic, would have supplied the heat source necessary for the crustal fusion.

By the studies carried to both – Borrachudos granites and metarhyolites from the southeastern Espinhaço Range, was shown that granitic magmas have been unlike formed during an orogenic episode. Instead, the geochronologic, petrologic, geochemical and isotopic data point to an anorogenic magma genesis context. On the basis of present data, is here propose an alternative tectonic model that better accounts for the nature of magmatic activity in the region.

After the Paleoproterozoic period of deformation and igneous activity between 2.2 to 1.9 Ga (Transamazonian event), the São Francisco craton and neighboring regions entered a period of quiescence regarding the compressional tectonics. However, at about 1.7 Ga, a stage of rifting started with deposition of the basal Espinhaço Supergroup, that is characterized by coarse-grained fluvial sediments and rare volcanic rocks (e.g. Dossin et al. 1990, Alkmim & Martins-Neto 2012, Chemale Jr. et al. 2012, Santos et al. 2013).

A broader subsidence with deposition of the upper transgressive fluvial to coastal shelf sequence that consists of quartzites, metasiltstones and shales, was followed by a stage of crustal fragmentation. During this time, the crust continued to undergo considerable modification involving deep-seated crustal melting leading to anorogenic intrusion, along the rift zone, of the epizonal K-rich BGS into the upper crust. Thus, the BGS constitutes a granitic magmatism event related to lithospheric thinning that led to the development of the Espinhaço rift in the Paleo- to Mesoproterozoic transition, and the furnished data indicate that this magmatism is fundamentally result of a crustal melting process occurring in response to asthenospheric uplift or upwelling of hot mantle material that compensated lithospheric thinning.

The period of Paleo- to Mesoproterozoic crustal extension showing similar sedimentary sequences with granitic magmatism associated has been described in other parts of the Brazilian shield (Pimentel et al. 1991, Amorim et al. 2021, Cruz et al. 2023). Continental-type acid magmatism related with extensive sedimentary sequences is known to the north of the Espinhaço Range in state of Bahia, where continental magmas intruded the cratonic basement in the Paramirim region, with granite intrusions around 1.73 Ga (U-Pb in zircon; Turpin et al. 1988), were coeval with the acid volcanism and associated tin-bearing greisens of the

Rio dos Remédios Group, the base unit of the Espinhaço Supergroup in this region.

An analogous case is represented to the west of the São Francisco Craton, in state of Goiás, where tin-bearing alkali-rich granites are coeval with metarhyolitic rocks from the basal part of the Araí Group, an extensive sedimentary succession of continental character possibly correlative with the Espinhaço Supergroup. Geochronological data for this association yielded ages of ~1.75 Ga (U-Pb in zircon; Pimentel et al. 1991, Tanizaki et al. 2015) to 1.58 Ga (Pb-Pb in zircon; Rossi et al. 1992).

The processes responsible for the profuse and widespread nature of synchronous magmatic episodes are not well understood. Some models regarding the problem that have been proposed include fusion induced by crustal thickening related to preceding orogenic episodes (Van Schmus & Bickford 1981), with mantle diapirism and crustal thinning leading to fusion by decompression of the lower crust (Anderson & Cullers 1978). In the Brazilian shield, the mechanism responsible for the formation of these and others possibly coeval magmatic provinces remains unclear. Without doubt, magmatism is a response to the development of extensive zones of fusion in the source. It is reasonable to suppose that mantle diapirism was related to these processes.

CONCLUSIONS

The BGS has all the distinctive mineralogical, petrological and geochemical features of A-type within-plate granites. The granites and metarhyolites have practically identical major and trace element contents, and similar Nd isotopic compositions, which are consistent with the assumption of a single source for these rocks. Trace elements and Nd-Sr isotopic compositions indicate that magmas were derived from partial melting of lower crust that was already depleted of first-batch melts related to the generation of early orogenic granitoid rocks during the Transamazonian event.

The processes of magma genesis were the result of crustal fusion as a consequence of the mantle upwelling related to lithospheric thinning in an anorogenic tensional regime, in contrast with other hypothesis regarding an orogenic origin. The petrological characteristics, chronology and geological context of emplacement of these rocks are identical to those of the other granitic provinces of the Brazilian shield.

The present tectonic model for the BGS is that magma genesis was related to lithospheric thinning that led to the development of the Espinhaço rift at about 1.7 Ga. The lithospheric thinning was compensated by asthenospheric uplift as demonstrated by the extensive generation of alkaline magmas. It is probable that upwelling of hot mantle material supplied the necessary energy to partial melting of the lower crust to yield the Borrachudos-type magma, which intruded the edges of the basin. Probably this period of crustal extension and associated igneous activity followed the Paleoproterozoic event (2.2-1.9 Ga), during which a large amount of new continental crust was formed by intrusion of I-type tonalites, granodiorites and granites.

BGS and other extend similar granitic provinces in the Brazilian shield can constitute belts of continental scale related to Paleo-Mesoproterozoic continental fracturing and formation of large basins, reflecting great rigidity of the continental crust after the thermotectonic phasis of probable Paleoproterozoic age. Overall occurrences can be characterized as anorogenic magmatism occurring whenever there was a resurgence of extension, rifting, deep melting and the provision of conduits for the mantle heat and mantle magmas to rise into and melt

the crust. There is no sufficient geochronological or paleomagnetic data to propose a geotectonic model to explain all similar occurrences, but could be speculate about the existence of a flatting mantle plume beneath a long protorift system in the period.

Acknowledgments

This work represents the development of studies of the doctoral thesis of the first author. The CNPq - Conselho Nacional de Desenvolvimento Tecnológico and CAPES – Coordenação de Aperfeiçoamento de Pessoal de Nível Superior Brazilian agencies, and the French and French-Brazilian programs COFECUB and URA.1366, supported the research. Many of the rock analyses had financial support from DOCEGEO – Rio Doce Geologia e Mineração (actual Vale Company). We are indebted to P. Vidal for isotopic analyses and review of the manuscript. The authors are grateful also to J.L. Robert and J. Pons for fruitful discussions.

REFERENCES

ALKMIM FF & MARTINS-NETO MA. 2012. Proterozoic first-order sedimentary sequences of the São Francisco craton, eastern Brazil. Mar Petr Geol 33: 127-139.

ALKMIM FF, KUCHENBECKER M, REIS HLS & PEDROSA-SOARES AC. 2017. The Araçuaí Belt. In: Heilbron M et al. (Eds.), São Francisco craton, eastern Brazil: tectonic genealogy of a miniature continent. Berlin: Springer, p. 255-276.

AMORIM LED, RIOS FJ, FREITAS ME, CUTTS K, GERALDES MC, DINIZ AD & MATOS EC. 2021. Zircon U-Pb geochronology of Paleoproterozic Statherian interplate A-type magmatic associations of the Lagoa Real uranium Province, São Francisco Craton (Bahia, Brazil). J South Am Earth Sci 109: 103245.

ANDERSON JL. 1983. Proterozoic anorogenic granite plutonism of North America. Geol Soc Am Bull 161: 133-152.

ANDERSON JL & BENDER E. 1989. Nature and origin of Proterozoic A-type granitic magmatism in the southwestern United States of America. Lithos 23: 19-52.

ANDERSON JL & CULLERS RL. 1978. Geochemistry and evolution of the Wolf River Batholit, a late precambrian rapakivi massif in North Wisconsin, USA. Precambrian Res 7: 287-324.

ANDERSON JL & MORRISON J. 1992. The role of anorogenic granites in the Proterozoic crustal development of North America. In: Condie KC (Ed.), Proterozoic Crustal Evolution, Dev Prec Geol, Elsevier, p. 263-291.

BRITO-NEVES BB, KAWASHITA K & DELHAL J. 1979. A evolução geocronológica da Cordilheira do Espinhaço: dados novos e integração. Rev Bras Geoc 9: 71-85.

CASSEDANNE JP, CASSEDANNE JO, ALVES JN & CARVALHO HF. 1995. Le pegmatite à aigue-marine de Ponte da Raiz et a paragênese Bi-Pb-(As) (municipe de Santa Maria de Itabira - Minas Gerais). An Acad Bras Cienc 67: 183-197.

CHAVES MLSC. 1997. Geologia e mineralogia do diamante da Serra do Espinhaço em Minas Gerais. PhD Thesis, University of São Paulo, Brazil, 289 p.

CHAVES MLSC, KARFUNKEL J, HOPPE A & HOOVER DB. 2001. Diamonds from the Espinhaço Range (Minas Gerais, Brazil) and their redistribution through the geologic record. Jour South Am Earth Sci 14: 277-289.

CHAVES MLSC, KARFUNKEL J & SVISERO DP. 1998. Lower Cretaceous conglomerates in the southern São Francisco basin, Minas Gerais: a model for the redistribution of ancient diamonds to cenozoic colluvial-alluvial deposits. An Acad Bras Cienc 70: 477-490.

CHAVES MLSC, PEDROSA-SOARES, AC, DUSSIN IA & MENEZES FILHO LA. 2024. Geocronologia U-Pb (LA-ICPMS) de zircões dos distritos pegmatíticos de Santa Maria de Itabira e São José da Safira (Minas Gerais): populações contrastantes na região da Província Pegmatítica Oriental do Brasil? Bol IG-USP, Sér Cient 24: 13-27.

CHEMALE JR F, DUSSIN IA, ALKMIM FF, MARTINS MM, QUEIROGA G, ARMSTRONG R & SANTOS MN. 2012. Unravelling a Proterozoic basin history through detrital zircon geochronology: the case of the Espinhaço Supergroup, Minas Gerais, Brazil. Gondwana Res 22: 200-206.

CHEMALE JR F, QUADE H & VAN SCHMUS WR. 1998. Petrography, geochemistry and geochronology of the Borrachudos and Santa Barbara metagranites, Quadrilátero Ferrífero, Brazil. Sbl Geol Paläont Teil I 3(6): 739-750.

CLEMENS JD & WALL VJ. 1981. Crystallization and origin of some peraluminous S-type granitic magmas. Can Min 19: 111-132.

COLLINS WJ, BEAMS SD, WHITE AJR & CHAPPELL BW. 1982. Nature and origin of A-type granites with particular references to southeastern Australia. Contrib Mineral Petr 80: 189-200.

CRUZ SCP, MACHADO GS, BARBOSA JSF, VITÓRIA RS, BARBOSA NS, NETO OVB, BITENCOURT CN, CRUZ VA & MARINHO MM. 2023. The Statherian anorogenic magmatism in the Paramirim

aulacogen, São Francisco-Congo paleoplate: new data, synthesis and regional correlations. J South Am Earth Sci 128: 104346.

CURRIE KL, EBY GN & GITTINS J. 1986. The petrology of the Mount Saint Hilaire complex, southern Quebec: an alkaline gabbro-peralkaline syenite association. Lithos 19: 67-83.

DE PAOLO DJ. 1981. A Nd and Sr isotopic study of the Mesozoic calc-alkaline granitic batholits of the Sierra Nevada and Peninsular Ranges, California. J Geophys Res 86: 10470-10488.

DORR II JV & BARBOSA ALM. 1963. Geology and ore deposits of the Itabira district, Minas Gerais, Brasil. US Geol Survey Prof Paper 341-C, 110 p.

DOSSIN IA, DOSSIN TM & CHAVES MLSC. 1990. Compartimentação estratigráfica do Supergrupo Espinhaço em Minas Gerais: os grupos Diamantina e Conselheiro Mata. Rev Bras Geoc 20: 178-186.

DUSSIN IA. 1994a. Evolution structurale de la partie méridionale de l'Espinhaço sur la bordure orientale du Craton São Francisco, Minas Gerais - Brésil: un exemple de tectonique protérozoïque superposé. PhD thesis, Universite d'Orléans, France, 200 p.

DUSSIN TM. 1994b. Associations plutono-volcaniques de l'Espinhaço méridional (SE-Brésil): un exemple d'évolution de la croûte protérozoïque. PhD thesis, Universite d'Orléans, France, 177 p.

EVENSEN NM, HAMILTON PJ & O'NIONS RK. 1978. Rare-earth abundances in chondritic meteorites. Geoch Cosmoch Acta 42: 1099-1112.

FAURE G. 1986. Principles of Isotope Geology. London: John Wiley & Sons, 589 p.

FERNANDES MLS, MARCIANO VR, OLIVEIRA RC, CORREIA-NEVES JM & DISLÁCIO MV. 1994. Granitos Borrachudos: um exemplo de granitogênese anorogênica na porção central do estado de Minas Gerais. Geonomos 2: 23-29.

GIRET A, BONIN B & LÉGER JM. 1980. Amphibole compositional trends in oversatured and undersatured alkaline plutonic ring-complexes. Can Min 18: 481-495.

GROSSI-SAD JH, CHIOD FILHO C, SANTOS JF, MAGALHÃES JMM & CARELO PM. 1990. Duas suítes graníticas do bordo sudeste do Craton Sanfranciscano, em Minas Gerais: petroquímica e potencial metalogenético. Proceed of the Congr Bras Geol 36: 1836-1848.

HEILBRON M, ALKMIM F & CORDANI U. 2017. The São Francisco Craton and its margins, Eastern Brazil. In: Heilbron M, Alkmim F, Cordani U (Eds.), São Francisco Craton, Eastern Brazil – Tectonic genealogy of a miniature continent. Berlin: Springer-Verlag, p. 3-13.

HERZ N. 1970. Gneissic and igneous rocks of the Quadrilátero Ferrífero, Minas Gerais, Brazil. US Geol Survey Prof Paper 641-B, 58 p.

JACOBSEN SB & WASSERBURG GJ. 1984. Sm-Nd isotopic evolution of chondrites and achondrites. J Earth Planet Sci Lett 67: 137-150.

JAVOY M & WEIS D. 1987. Oxygen isotopic composition of alkaline anorogenic granites as a clue to their origin: the problem of the crustal oxygen. Earth Planet Sci Lett 84: 415-422.

JORDT-EVANGELISTA H, LANA C, DELGADO CER & VIANA DJ. 2016. Age of the emerald mineralization from the Itabira-Nova Era District, Minas Gerais, Brazil, based on LA-ICP-MS geochronology of cogenetic titanite. Braz J Geol 46: 427-437.

KANIG M. 1985. Die Verteilung von Haupt-und Spurenelementen in lateristischen Boden uber granitischen Gesteine, Borrachudos, Santa Bárbara (Minas Gerais, Brasilien). Master thesis, Inst. Min. Largest, Aachen, Germany, 129 p. (Unpublished).

LEAKE BE. 1978. Nomenclature of amphiboles. Can Min 16: 501-520.

LINDSLEY DH. 1976. Experimental studies of oxide minerals. In: D. Rumble (Ed.), Oxide Minerals. Mineral Soc Am Short Course Notes 3: L61-L84.

LOISELLE MC & WONES DR. 1979. Characteristics and origin of anorogenic granites. Geol Soc Am Abst Prog 11: 468.

LONDON D. 2008. Pegmatites. Québec: Can Min Spec Publ 10, 346 p.

MAALφE S & WYLLIE PJ. 1975. Water content of a granite magma as deduced from the sequence of crystallization determined experimentally with water-undersaturated conditions. Contrib Mineral Petrol 52: 175-191.

MACHADO N, SCHRANK A, ABREU FR, KNAUER LG & ALMEIDA-ABREU PA. 1989. Resultados preliminares da geocronologia U/Pb na Serra do Espinhaço Meridional. Proceed of the Simp Geol Minas Gerais 5: 171-174.

MANIAR PD & PICCOLI PM. 1989. Tectonic discrimination of granitoids. Geol Soc America Bull 101: 635-643.

MARTIN RF. 1988. The feldspar mineralogy of granites and rhyolites: a generalized case pseudomorphism of the magmatic phase. Rend Soc Ital Mineral Petrol 43(2): 343-354.

NETTO C, ARAÚJO MC, PINTO CP & DRUMOND JBV. 1998. Projeto Leste – Cadastramento de Recursos Minerais - Pegmatitos. Belo Horizonte: CPRM-COMIG, 223 p.

NOCE CM, TEIXEIRA W, QUÉMÉNEUR JJG, MARTINS VTS & BOLZACHINI E. 2000. Isotopic signatures of paleoproterozoic granitoids from the southern São Francisco Craton and implications for the evolution of the Transamazonic Orogeny. J South Am Earth Sci 13: 225-239.

PEARCE JA, HARRIS NBW & ANDREW GT. 1984. Trace element discrimination diagrams for the tectonic interpretation of granitic rocks. J Petrol 25: 956-983.

PEDROSA-SOARES AC ET AL. 2011. Late Neoproterozoic–Cambrian granitic magmatism in the Araçuaí orogen (Brazil) the Eastern Brazilian Pegmatite Province and related mineral resources. Geol Soc London Spec Publ 350: 25-51.

PIMENTEL M, HEAMAN L, FUCK RA & MARINI OJ. 1991. U-Pb zircon geochronology of Precambrian tin-bearing continental-type acid magmatism in central Brazil. Precambrian Res 52: 321-335.

PINTO CP & SILVA MA. 2014. Mapa Geológico do Estado de Minas Gerais Escala 1:1.000.000. Belo Horizonte: CODEMIG-CPRM.

PUPIN JP. 1980. Zircon and granite petrology. Contrib Mineral Petrol 73: 207-220.

ROBERT JL. 1976a. Phlogopite solid solutions in the system K_2O-MgO-Al_2O_3-SiO_2-H_2O. Chem Geol 17: 195-212.

ROBERT JL. 1976b. Titanium solubility in synthetic phlogopite solid solutions. Chem Geol 17: 213-227.

ROBERT JL & MAURY RC. 1979. Natural occurrence of a (Fe, Mn, Mg) tetrasilic potassium mica. Contrib Mineral Petrol 68: 117-123.

ROSSI P, ANDRADE GF & COCHERIE A. 1992. The 1.58 Ga A-type granite of Serra da Mesa (GO): an example of "NYF" fertile granite pegmatite. Proceed of the Congr Bras Geol 37: 389-390.

SANTOS MN, CHEMALE JR F, DUSSIN IA, MARTINS M, ASSIS TR, JELINEK AR, GUADAGNIN F & ARMSTRONG R. 2013. Sedimentological and paleoenvironmental constraints of the Statherian and Stenian Espinhaço rift system, Brazil. Sed Geol 290: 47-59.

SEIFERT F & SCHREYER W. 1971. Synthesis and stability of micas in the system K_2O-MgO-SiO_2-H_2O and their relations to phogopite. Contrib Mineral Petrol 30: 196-215.

SIGA JR. O. 1986. A evolução geotectônica da porção nordeste de Minas Gerais, com base em interpretações geocronológicas. Master thesis, São Paulo University, Brazil, 140 p. (Unpublished).

STRECKEISEN A. 1976. To each plutonic rocks its proper name. Earth Sci Rev 12: 1-33.

TAYLOR RP, STRONG DF & KEAN BF. 1980. The Topsails igneous complex: Silurian-Devonian peralkaline magmatism in western Newfoundland. Can J Earth Sci 17: 425-439.

TANIZAKI MLN, CAMPOS JEG & DARDENNE MA. 2015. Estratigrafia do Grupo Araí: registro de rifteamento paleoproterozoico no Brasil Central. Braz J Geol 45: 95-108.

TEIXEIRA W, DUSSIN IA, DUSSIN TM, SALVADOR ED, SIGA JR O & SATO K. 1990. Interpretação do contexto geotectônico do embasamento na borda leste do sistema Espinhaço, região de Guanhães e Gouveia-MG, com base numa integração do seu conjunto geocronológico U/Pb, Rb/Sr e K/Ar. Proceed of the Cong Bras Geol 36(6): 2711-2722.

TEIXEIRA W & FIGUEIREDO MCH. 1991. An outline of Early Proterozoic crustal evolution in the São Francisco craton, Brazil: a review. Precambrian Res 53: 1-22.

TURPIN L, MARUEJOL P & CUNEY M. 1988. U-Pb, Rb-Sr and Sm-Nd chronology of granitic basement, hydrotermal albitites and uranium mineralization (Lagoa Real, south Bahia, Brazil). Contrib Mineral Petrol 98: 139-147.

UHLEIN A. 1991. Transição Cráton - Faixa dobrada: um exemplo do Cráton São Francisco e da Faixa Araçuaí (Ciclo Brasiliano) no Estado de Minas Gerais. PhD thesis, São Paulo University, Brazil, 295 p.

VAN SCHMUS WR & BICKFORD ME. 1981. Proterozoic chronology and evolution of the midcontinent region, North America. In: Kroner A (Ed.), Precambrian Tectonic Plates, Amsterdam: Elsevier, p. 261-296.

WHALEN JB, CURRIE KL & CHAPPELL BW. 1987. A-type granites: geochemical characteristics, discrimination and petrogenesis. Contrib Mineral Petrol 95: 407-419.

How to cite

DUSSIN IA, CHAVES MLSC, DUSSIN TM, ROSSI P & CHARVET J. 2025. The Borrachudos Granitic Suite: Paleo- to Mesoproterozoic A-type Magmatism in the Southeastern São Francisco Craton (SE Brazil). An Acad Bras Cienc 97: e20231253. DOI 10.1590/0001-3765202520231254.

Manuscript received on November 14, 2023;
accepted for publication on October 23, 2024

IVO ANTONIO DUSSIN[1]
https://orcid.org/0000-0002-5205-5359

MARIO LUIZ S.C. CHAVES[1]
https://orcid.org/0000-0002-8486-9074

TANIA MARA DUSSIN[2]
https://orcid.org/0009-0001-5153-9597

PHILLIPPE ROSSI[3]
https://orcid.org/0000-0003-1245-2752

JACQUES CHARVET[4]
https://orcid.org/0000-0002-3553-5692

[1]Universidade do Estado do Rio de Janeiro,
Faculdade de Geologia, Rua São Francisco Xavier
524,20550-900 Rio de Janeiro, RJ, Brazil

[2]Universidade Federal de Minas Gerais, Instituto de
Geociências, Campus da Pampulha, Avenida Antônio
Carlos 6627, 31270-901, Belo Horizonte, MG, Brazil

[3]Bureau de Recherches Géologiques et
Minières, BP 6009, 45060 Orléans, France

[4]Université d'Orléans, Laboratoire de Géologie Structurale,
URA/CNRS, GDR 969, BP 6759, 45067 Orléans, France.

Correspondence to: **Mario Luiz Sá Carneiro Chaves**
E-mail: sacarneiro.70@gmail.com

Author contributions

IVO ANTONIO DUSSIN: Introduction, BGS Previous Knowledge, Regional Tectonic Evolution, Concluding Remarks, Results. MARIO LUIZ S.C. CHAVES: Introduction, BGS Previous Knowledge, Regional Tectonic Evolution, Concluding Remarks. TANIA MARIA DUSSIN: Results. PHILLIPPE ROSSI and JACQUES CHARVET: Results, Petrogenetic Discussions.